Supporting Information

Hussain *et al.* 10.1073/pnas.0802928105

SI Text

Section A: Analytical Expressions for the Three-Step Mechanism of Cu Transfer. Our derivation is based on the following reaction scheme:

$$PX + L \underset{k_{-1}}{\overset{k_1}{\rightleftharpoons}} PXL \underset{k_{-2}}{\overset{k_2}{\rightleftharpoons}} P + XL + L \underset{k_{-3}}{\overset{k_3}{\rightleftharpoons}} LXL, \qquad \textbf{[S1]}$$

where P = Atox1, L = BCA, and X = Cu^{1+}.

A1. First, an expression for the equilibrium change in absorption was derived as function of [BCA or L], [$Atox1_{free}$ or P], and K_1–K_3. The fraction of Cu in the colored LXL complex Y_{LXL} is given by the ratio of (LXL) and the total concentration of Cu species present in the mixture (i.e., LXL, PX, PXL, XL):

$$Y_{LXL} = \frac{[LXL]}{[PX] + [PXL] + [XL] + [LXL]}. \qquad \textbf{[S2]}$$

When fitting the experimental amplitude data at different [BCA], Y_{LXL} was multiplied with the maximum change in absorbance detected experimentally, ΔA_{max}, to obtain the fitted ΔA vs. $[BCA]_{free}$. The relative concentrations of the copper-containing species are defined by the equilibrium constants for steps, 1, 2, and 3:

$$K_1 = \frac{[PXL]}{[PX][L]} \quad K_2 = \frac{[LX][P]}{[PXL]} \quad K_3 = \frac{[LXL]}{[LX][L]}.$$

These expressions were used to define the relative probabilities of PX, PXL, XL, and LXL in Eq. S2 in terms of [P], [L], K_1, K_2, and K_3:

$$Y_{LXL} = \frac{K_1K_2K_3[L]^2}{[P] + K_1[L][P] + K_1K_2[L] + K_1K_2K_3[L]^2}. \qquad \textbf{[S3]}$$

The theoretical absorbance changes were computed as $\Delta A_{max} \times Y_{LXL}$. Fits to the observed data were obtained by optimizing the K values to minimize the sum of the squared differences between the observed and calculated absorbance differences by using the Solver function in Microsoft Excel 2004 version 11.7.3

A2. To obtain an expression for the observed first order rate constant for Cu displacement from Atox1 as a function of [BCA], we started with the rate equations for the formation of colored product, LXL, while making steady state assumptions for the PXL and XL intermediates. The rate of decay of the initial species, PX and the final product, LXL, is given by:

$$-\frac{d[PX]}{dt} = \frac{d[LXL]}{dt} = k_3[L][XL] - k_{-3}[LXL];$$

because $[LXL] = X_0 - ([PX] + [PXL] + [XL])$, we can rearrange to:

$$-\frac{d[PX]}{dt} = (k_3[L] + k_{-3})[XL] + k_{-3}[PX] + k_{-3}[PXL] - k_{-3}X_0. \qquad \textbf{[S4]}$$

To obtain a simple linear first order differential equation in [PX] (or [LXL]), we need expressions for [XL] and [PXL] in terms of X_0 and [PX]. To obtain expressions for [XL] and [PXL], the steady-state assumption was applied to these species, i.e., their absolute values and rate of changes are ≈0.

A2a. We first derived an expression for [PXL] in terms of [PX], [L], [P], and [XL]:

$$\frac{d[PXL]}{dt} = k_1[L][PX] + k_{-2}[P]\cdot[XL] - (k_{-1} + k_2)[PXL] = 0$$

$$0 = k_1[L][PX] + k_{-2}[P]\cdot[XL] - (k_{-1} + k_2)[PXL]$$

$$[PXL] = \frac{k_1[L][PX] + k_{-2}[P]\cdot[XL]}{(k_{-1} + k_2)}.$$

A2b. Next, an expression for [XL] was derived by using the expression for [PXL]:

$$\frac{d[XL]}{dt} = k_2[PXL] + k_{-3}[LXL] - (k_{-2}[P] + k_3[L])[XL] = 0; \qquad [LXL] = X_0 - ([PX] + [PXL] + [XL]).$$

The expression for [*XL*] was obtained from the equation above. By using our earlier expression for [*LXL*] and that for [*PXL*], we can rearrange the expression above to become:

$$[XL] = \frac{(k_2k_1[L] - ((k_{-3}k_{-1} + k_{-3}k_2) + k_{-3}k_1[L]))[PX]}{((k_{-3}k_{-2} + k_{-2}k_{-1})[P] + (k_{-3}k_{-1} + k_{-3}k_2) + (k_3k_{-1} + k_3k_2)[L])}$$

$$+ \frac{(k_{-1} + k_2)k_{-3}X_0}{((k_{-3}k_{-2} + k_{-2}k_{-1})[P] + (k_{-3}k_{-1} + k_{-3}k_2) + (k_3k_{-1} + k_3k_2)[L])}.$$

A2c. The expressions for [*XL*] and [*PXL*] were then inserted into Eq. S4, the rate equation for −d[*PX*]/dt. This differential equation is linear first order and can be arranged into the following form:

$$\frac{d[PX]}{dt} = -R(L, P, k_x)\cdot[PX] + Q(L, P, k_x, X_0),$$

where $R(L,P,k_x)$ and $Q(L,P,k_x, X_0)$ are functions of the rate constants, and [*L*], [*P*], and X_0 are the total Cu concentration. For this type of linear first order differential equation, the final solution for the observed pseudo first order rate constant k_{obs} will be $R(L,P,k_x)$.

After insertion of the expressions for the [*XL*] and [*PXL*] into Eq. S4 and rearranging, the final expression for $R(L,P,k_x)$ or k_{obs} is:

$$k_{obs} = \frac{k_{-3}k_{-2}(k_{-3} + k_{-1})[P] + k_1k_2k_{-3}[L] + k_1k_{-2}k_{-3}[L][P] + k_1k_2k_3[L]^2}{k_{-2}(k_{-3} + k_{-1})[P] + k_{-3}(k_{-1} + k_2) + k_3(k_{-1} + k_2)[L]}. \quad \textbf{[S5]}$$

A2d. Eq. S5 predicts the following values of k_{obs} at the two limiting conditions.

When L → 0 and [P] → infinity, k_{obs} will become equal to k_{-3}. Thus, Eq. S5 predicts that there should be little dependence of the *y* intercept on [*P*] for plots of k_{obs} vs. [BCA] as long as the protein concentration is reasonably large.

$$k_{obs} \approx \frac{k_{-3}k_{-2}(k_{-3} + k_{-1})[P]}{k_{-2}(k_{-3} + k_{-1})[P]} \approx k_{-3} \quad \textbf{[S6]}$$

When L → ∞, then the observed rate constant will increase linearly in [*L*] and the apparent bimolecular rate constant will equal:

$$k_{obs} \approx \frac{k_1k_2k_3[L]^2}{k_3(k_{-1} + k_2)[L]} \approx \frac{k_1k_2[L]}{(k_{-1} + k_2)} \quad \textbf{[S7]}$$

Fits in Figs. 3 and 4 were obtained by fitting sets of both equilibrium absorbance changes and k_{obs} vs. [BCA] data globally. Again, the sum of squared errors was minimized by varying the three equilibrium constants and each of the reverse rate constants, k_{-1}, k_{-2}, k_{-3}, by using the Solver tool in Microsoft Excel. The forward rate constants were defined by the equilibrium constants and the reverse rate constants (i.e., $k_1 = K_1 \times k_{-1}$). The maximum absorbance changes for the equilibrium data were also varied.

The derivations above only apply rigorously to pseudo first order conditions, which imply simple exponential time courses. The conditions for the kinetic BCA experiments with 3.6 μM apo-Atox1 and 3.3 μM Cu (Fig. 4) are non-pseudo first order with respect to [*P*]. For the fitting procedures, we used free [*P*] = 2 μM in these cases. This was estimated from the formula for 50% binding: then free [*P*] = 3.6 − 3.3/2 = 2.0 μM. We note that at high BCA, where 100% Cu transfer occurs, free [*P*] will approach 3.6 μM, but at $t_{1/2}$ the value will still be 2.0 μM; however, at low BCA, where little Cu binding occurs, free [*P*] at the end of the reaction will be smaller than 2 μM. For the higher [*P*] concentrations (i.e., 9 and 15 μM), we have approximate pseudo first order conditions with respect to excess [*P*]. The fact that all three sets of data at 3.6, 9.0, and 15 μM Atox1 and 3.3 μM Cu could be fitted well to equations S2 and S5 (Figs. 3 and 4) suggests strongly the deviation from pseudo first order condition at the lower protein concentration has little effect on our analyses.

Section B: Alternative Two-Step Reaction Schemes for Cu Displacement from Atox1. We also compared the analytical expressions for three distinct two-step mechanisms. The same derivation approach was used. The definition of Y_{LXL} was [*LXL*]/X_0 where X_0 is the total concentration of Cu. Steady state assumptions were made for the intermediate to obtain a linear first order differential equation. The final expressions for Y_{LXL} and k_{obs} are listed under each mechanism.

B1. Two-step mechanism starting with Atox1 monomer:

$$PX + L \underset{k_{-1}}{\overset{k_1}{\rightleftharpoons}} PXL + L \underset{k_{-2}}{\overset{k_2}{\rightleftharpoons}} P + LXL,$$

where *P* = Atox1, *L* = BCA, and *X* = Cu^{1+}.

By using the same approach as for the 3-step mechanism, we obtained the following equilibrium and kinetic expressions:

B1a. Equilibrium expression:

$$Y_{LXL} = \frac{K_1K_2[L]^2}{[P] + K_1[L][P] + K_1K_2[L]^2}$$

B1b. Kinetic expression:

$$k_{obs} = \frac{k_{-1}k_{-2}[P] + k_1k_{-2}[L][P] + k_1k_2[L]^2}{k_{-2}[P] + k_{-1} + k_2[L]}$$

The limiting values of k_{obs} are similar in form to those for the 3-step scheme.

$$\text{When } [P] \rightarrow \infty \text{ and } [L] \rightarrow 0,\ k_{obs} \rightarrow k_{-1}$$

$$\text{When } [P] \rightarrow 0 \text{ and } [L] \rightarrow \infty,\ k_{obs} \rightarrow k_1[L]$$

The *y axis* intercept has a different meaning in this mechanism as compared to the 3-step mechanism. Here, the *y* axis intercept is the rate of dissociation of the first BCA from the Atox1-Cu-BCA complex and should vary with mutation of Atox1.

B1c. Simultaneous fits of equilibrium and kinetic data for wild-type Atox1 at three different [*P*] concentrations to the expressions derived for the two-step scheme are shown in Fig. S1 and are almost as good as those for the three step scheme. Table S1 reports the values extracted from these fits.

B2. Two-step scheme with Atox1-Cu dissociation followed by BCA binding (original idea):

$$PX \underset{k_{-1}}{\overset{k_1}{\rightleftharpoons}} P + X + 2L \underset{k_{-2}}{\overset{k_2}{\rightleftharpoons}} LXL,$$

where P = Atox1, L = BCA, and X = Cu^{1+}.

B2a. Equilibrium expression:

$$Y_{LXL} = \frac{K_1K_2[L]^2}{[P] + K_1 + K_1K_2[L]^2}.$$

B2b. Observed rate expression:

$$k_{obs} = \frac{k_{-1}k_{-2}[P] + k_1k_{-2} + k_1k_2[L]^2}{k_{-1}[P] + k_{-2} + k_2[L]^2}.$$

The limiting values are:

$$\text{When } [L] \rightarrow 0 \text{ and [P]} \rightarrow \text{infinity},\ k_{obs} \approx k_{-2}$$

$$\text{When } [L] \rightarrow \infty,\ k_{obs} \rightarrow k_1$$

This mechanism predicts that the y-intercept will equal k_{-2} (rate of first BCA dissociation from the BCA-Cu-BCA complex) and that as $[L] \rightarrow \infty$ k_{obs} will equal k_1, the rate of dissociation of Cu from Atox1-Cu. Thus, there should be a limiting rate at high [*L*], which *is not experimentally observed*.

B2c. Simultaneous fits of the equilibrium and kinetic data for wild-type Atox1 at three different [*P*] concentrations to the expressions derived for this two-step, dissociation-first scheme, are shown in Fig. S2. Table S2 reports the values extracted from these fits.

The poor fit to the kinetic data demonstrates that simple Atox1-Cu dissociation is not the first step in the reaction. BCA must be reacting directly with Atox1-Cu to facilitate Cu displacement. This simple dissociation mechanism cannot predict a parabolic dependence of k_{obs} on [BCA].

B3: Two-step scheme starting with Atox1 dimer (*PXP*). This mechanism was considered because Atox1 was crystallized as a homodimer bridged by a single Cu ion; thus, it is possible that Atox1 dimers exist in solution. However, analytical ultracentrifuge experiments appear to rule out Aotx1 dimers in our solutions (see main text).

$$PXP + L \underset{k_{-1}}{\overset{k_1}{\rightleftharpoons}} P + PXL + L \underset{k_{-2}}{\overset{k_2}{\rightleftharpoons}} P + LXL,$$

where P = Atox1, L = BCA, and X = Cu^{1+}.

B3a. The equilibrium expression becomes:

$$Y_{LXL} = \frac{K_1K_2[L]^2}{[P]^2 + K_1[L][P] + K_1K_2[L]^2}.$$

B3b. The kinetic rate expression becomes:

$$k_{obs} = \frac{k_1k_2[L]^2 + k_1[L]k_{-2}[P] + k_{-1}k_{-2}[P]^2}{(k_{-1} + k_{-2})[P] + k_2[L]}$$

The limiting values are:

$$\text{When } [L] \rightarrow 0,\ k_{\text{obs}} = \frac{k_{-1}k_{-2}[P]}{k_{-1} + k_{-2}}$$

$$\text{When } [L] \rightarrow \infty,\ k_{\text{obs}} = k_1[L]$$

This mechanism predicts that the y-intercept will depend linearly on [Atox1], which is not observed.

B3c. Simultaneous fits of the equilibrium and kinetic data for wild-type Atox1 at three different [*P*] concentrations to the expressions derived for the dimer two-step scheme are shown in Fig. S3. Table S3 reports the values extracted from these fits. These poor fits to the kinetic data demonstrate that there are no Atox1 dimers under the conditions used and that the Cu complex acts as a monomer kinetically.

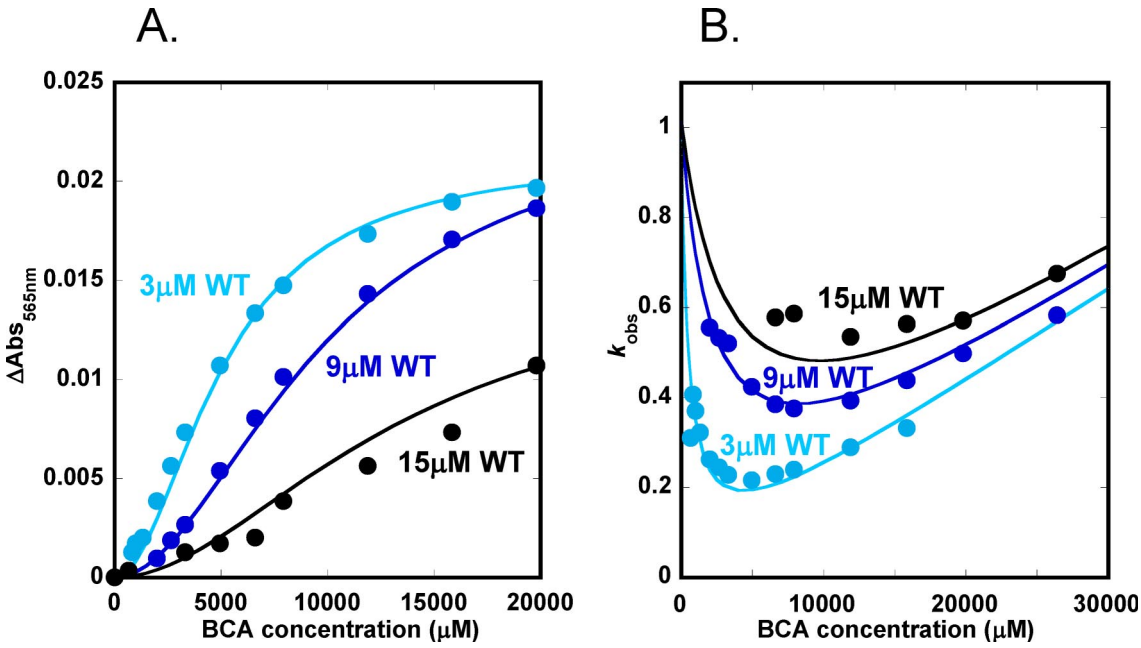

Fig. S1. Fits to amplitude (*Left*) and rate (*Right*) data for three wild-type Atox1 concentrations based on the two-step monomer mechanism.

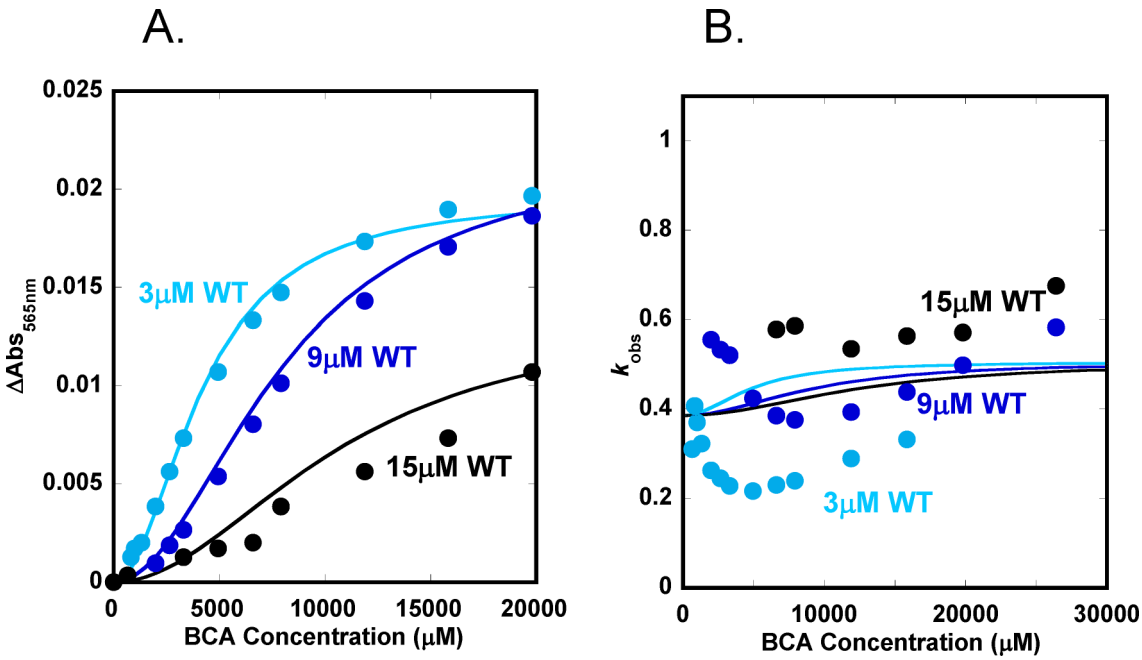

Fig. S2. Fits to amplitude (*Left*) and rate (*Right*) data for three wild-type Atox1 concentrations based on the two-step Cu dissociation-first mechanism.

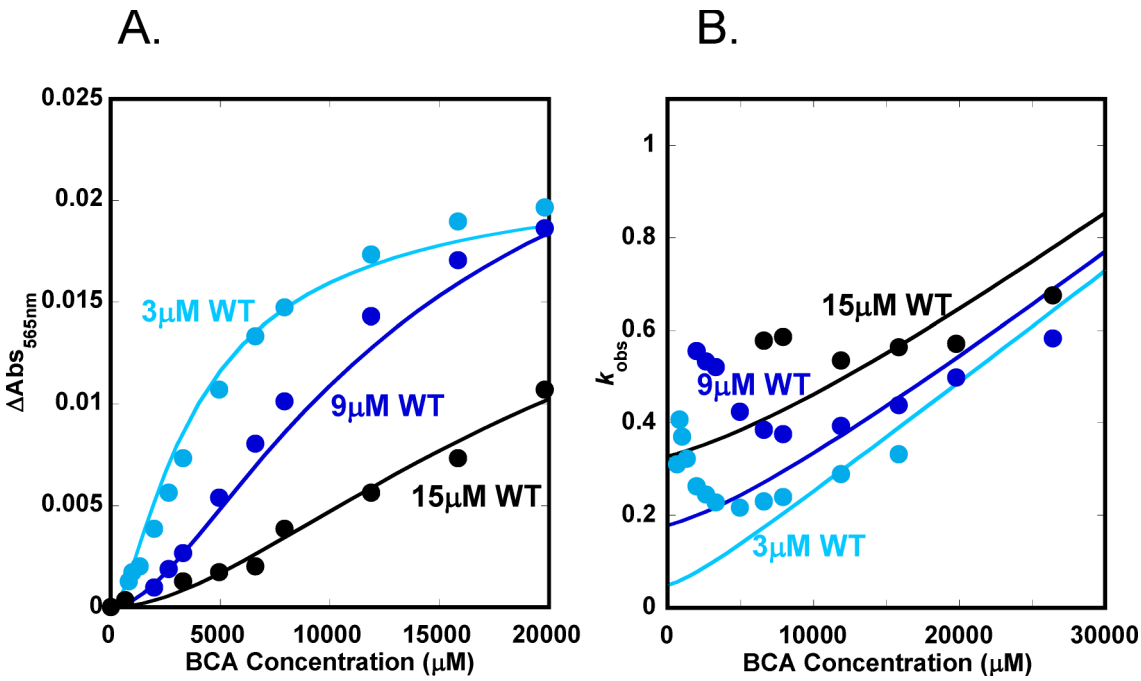

Fig. S3. Fits to amplitude (*Left*) and rate (*Right*) data for three wild-type Atox1 concentrations based on the two-step Atox1 dimer mechanism.

Table S1. Summary of equilibrium and kinetic parameters obtained from global fitting of amplitude and rate data for Atox1 (Figure S1) based on the two-step monomer mechanism.

K_1, μM^{-1}	K_2	k_1, $\mu M^{-1}s^{-1}$	k_{-1}, s^{-1}	k_2, $\mu M^{-1}s^{-1}$	k_{-2}, $\mu M^{-1}s^{-1}$
2.0×10^{-5}	4.1×10^{-3}	2.1×10^{-5}	1.0	4.1×10^{-2}	10.0

Table S2. Summary of equilibrium and kinetic parameters obtained from global fitting of amplitude and rate data for Atox1 (Figure S2) based on the two-step, dissociation-first mechanism

K_1, μM	K_2, μM^{-2}	k_1, s^{-1}	k_{-1}, $\mu M^{-1}s^{-1}$	k_2, $\mu M^{-2}s^{-1}$	k_{-2}, s^{-1}
6.3×10^{-5}	1.8×10^{-3}	5.1×10^{-1}	8.0×10^{3}	7.0×10^{-4}	3.9×10^{-1}

Table S3. Summary of equilibrium and kinetic parameters obtained from global fitting of amplitude and rate data for Atox1 (Figure S3) based on the two-step dimer mechanism

K_1	K_2	k_1, $\mu M^{-1}s^{-1}$	k_{-1}, $\mu M^{-1}s^{-1}$	k_2, $\mu M^{-1}s^{-1}$	k_{-2}, $\mu M^{-1}s^{-1}$
9.6×10^{-4}	6.0×10^{-4}	2.4×10^{-5}	2.5×10^{-2}	4.7×10^{-4}	7.4×10^{-1}